FATIGUE FRACTURE ROUGHNESS CHARACTER AFTER PLASMA NITRIDING PROCESS

STUDENY Zbynek[1], SURLAKOVA Maria[2], CHLEBINOVA Lenka[2]

[1]*University of Defence in Brno, Czech Republic, EU, zbynek.studeny@unob.cz*
[2]*Alexander Dubček University of Trenčín, Faculty of Special Technology, Slovakia, EU*

Abstract

In this study, the cyclic loading of steel samples 41CrAlMo7-10 (1.8509) were made. This steel is suitable for plasma nitriding proces. The experiment included 4 different plasma nitriding procedures. The differences were applied in plasma nitriding atmosphere and procedure duration. Then follow-up a fatigue test. The fatigue tests were carried out in accordance with the CSN 42 0363 Fatigue Testing of Metals, Methodology of Testing in the machine R.R.Moore L2568 of Instron Co. Fatigue tests were compiled graphically and numerically using Wöhler`s (S-N) curve in a semi-logarithmic form. The testing was stopped after reach the fracture of tested sample or after 107 cycles. Area of study was fatigue fracture. Specifically, part of fatigue fracture around inclusions and their vicinity. This part is known as fish-eye and has specific shape and morphology in terms of surface topography. The surface topography of fatigue cracks were evaluated on Talysurf CCI. Roughness parameters were tested in this area at six defined lines from fatigue crack initiation.

Keywords: Plasma nitriding, inclusion, fish-eye

1. INTRODUCTION

Although the fatigue of metals under the cyclic mechanical loads is known since the beginning of the railway lines, the reasons for its growth have not yet been sufficiently analysed. Growing demands on the mechanical properties of structural materials, downsizing, increasing the speed and forces acting on structure-borne components and effects of the environment are the reason why attention is to be paid to the fatigue of materials [1]. The subject is not only solution to consequences but actions and processes to investigate causes that lead ultimately to failure of key components. Therefore, the consequences are varied.

It is known that plasma nitriding process provides improved fatigue characteristics [2]. The reasons are both in the surface layer hardness and in the nature of the growing stress, which to some extent successfully averts propagation of a fatigue crack [3]. Once the stress intensity exceeds some limit value, stress accumulates in the vicinity of an inclusion and fatigue crack develops. In terms of crack development, an inclusion has to be found at the interface of the diffusion layer and the base material. With steel 41CrAlMo7-10 (1.8509) investigated herein, a visually and topographically delimited fish-eye ellipse reaches a width of 300 μm to 600 μm and a depth of approximately 200 μm to 400 μm [4,5]. Seeing that the depths of the diffusion layers are within the range of 250 μm to 350 μm, depending on processing formulas applied, a fish-eye is to be found at interface between the diffusion layer and the base material. This has an effect on a dissimilar fatigue crack growth due to different physical parameters of the nitride diffusion layer on the one side, and the base material on the other [6]. Using Talysurf CCI Lite, first of all assess the surface roughness at defined distance levels from the inclusion site, as a rule located in the vicinity of the interface of diffusion layer and the base material. The interface is not sharply defined, so the term 'located in the vicinity' for an inclusion is appropriate here. A 3D model has been set up based on the measured data of the investigated fish-eye area, which was analysed.

2. DEFINING THE INVESTIGATIONAL MATERIAL

The material used for the 3-point bending rotation testing was 41CrAlMo7-10 steel (1.8509). Specimens of the steel were prepared according to the test specification criteria. Machining was carried out so as to avoid undercuts that would behave as stress concentrators and impair the test. The specimens were divided into five sets and heat-treated. The treatment consisted of: normalizing (900°C; 25'; air cooling), tempering (930°C; 25'; cooling in oil) and tempering (640°C; 40'; cooling in oil) [7].

Only 4 series were used for the subsequent surface treatment by a plasma nitriding formula. The process was carried out on Rübig PN 60/60 at 500°C for all series. The fifth series remained as a reference for determining the expected increase in fatigue characteristics [8, 9]. Plasma nitriding procedure and the resultant depth of the white and diffusion layer are evident from **Table 1**.

Table 1 Plasma nitriding process and results of white and diffusion layer depth

Series	Time [h]	Atmosphere (H_2:N_2) Flow rate [l/h]	White layer depth [μm]	Diffusion layer depth [μm]
PN1	10	8:24	5.2 ± 1	**264**
PN2	20	8:24	8.7 ± 1	**344**
PN3	10	24:8	1.9 ± 0.5	**227**
PN4	20	24:8	1.9 ± 0.3	**304**

3. CONDUCTING THE EXPERIMENT

The fatigue tests of all sample series were conducted on Instron R. R. Moore rotating beam fatigue testing system. This was a 3-point rotating bending at constant stress of amplitude σ_a and constant speed. The test procedure was in accordance with CSN 42 0363 [10]. Evaluation of the measured results and the deriving of Wöhler's curves (SN-curves) were done in accordance with the CSN 42 0368 [11]. The fractures obtained were investigated from the viewpoint of surface topography on Talysurf CCI Lite mutual coherence correlation interferometry. Of all fracture parts, attention was focused mainly on the fish-eye, typical of the plasma nitrided components under cyclic loading. Arithmetic mean deviation of the roughness profile Ra indicated in μm was applied to evaluate the measured values of surface roughness and waviness [12]. The system measuring face setting corresponded to the fish-eye area to be measured. The zoom value of the lens used was 20x, whereby the real measuring face area was 0.8x0.8 mm, see **Figure 1**. The above lens can achieve accuracy of about 0.01 nm when roughness is measured within a range of 2.2 mm in Z-axis [13].

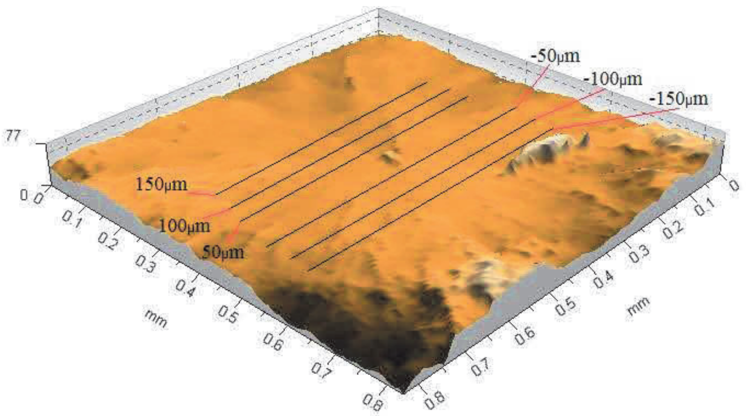

Figure 1 3-D model with outlined planes to assess the fish-eye topography

A spatial model, **Figure 1**, of the fisheye outlined planes where the measurement of roughness parameters took place. These planes were divided into two groups of three levels. An inclusion has been chosen there as the centre, around which the measurement was conducted. One group was above the inclusion towards the diffusion layer, the other group was under inclusion oriented to the base material. The orientation of the measurement planes was parallel to the sample surface. The spacing between the inclusion and the separate measurement planes was 50 μm.

4. DISCUSSING THE RESULTS

The fatigue test results by means of the 3-point rotating bending were processed and evaluated in accordance with the CSN 42 0368 [11]. The values were approximated by the straight-line equation:

$$\log\sigma_a = A + B.\log N_f. \quad (1)$$

The fatigue S-N-curves were determined by subsequent regression analysis according to the equation:

$$\sigma_a = \sigma_{f'}(2N_f)^b \quad (2)$$

Figure 2 shows the resulting curves in semi logarithmic form σ_a - log N_f. **Table 2** presents the values of the ultimate strength with the equations of the inclined parts of S-N curves obtained by linear regression according to equation (2) and the reliability value R^2 of the series PN1 to PN4. If the samples exceeded 10^7 cycles and fracture did not show up, the experiment was stopped in accordance with the CSN 42 0363 [10].

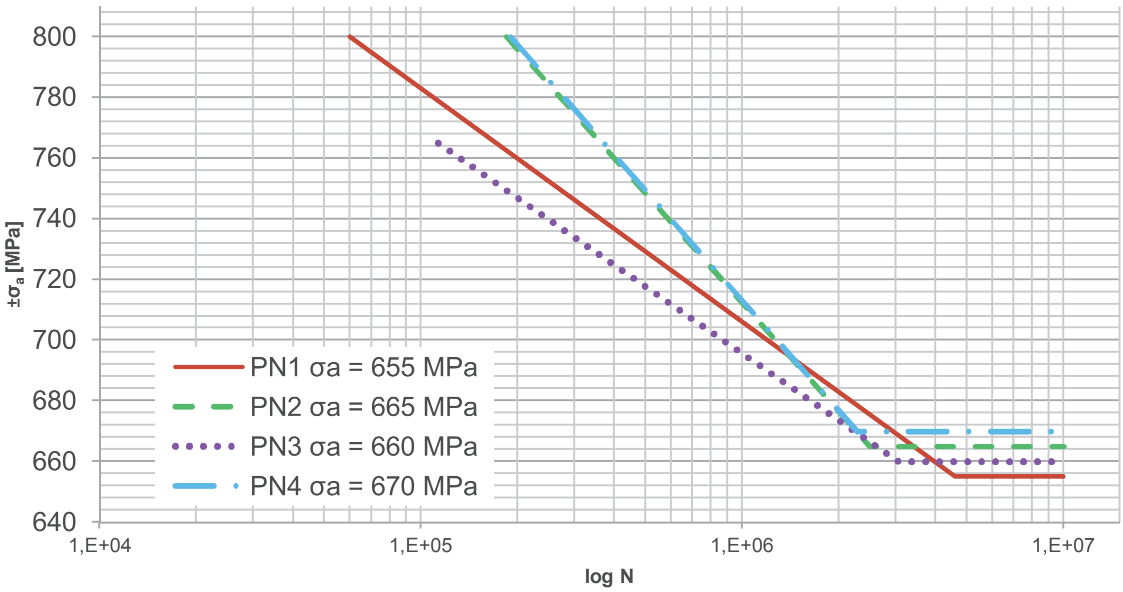

Figure 1 SN-curves of the plasma nitrided samples in PN1 to PN4 procedures

The S-N curves in **Figure 2** show that the extended plasma nitridation procedure in both types of atmospheres resulted in permanent fatigue strength increases. Although the atmosphere in PN4 series is poorer in nitrogen, if compared to PN2 series, which, according to **Table 1**, results in the thinner diffusion layer on the one side, but also in the thinner white layer on the other. The heterogeneous white layer is very hard and thus a likely source of a network of cracks [13, 14].

Table 2 Fatigue test results

Series	Fatigue strength σ_a [MPa]	Regression equation	Reliability value
PN1	655	y = -32.3ln(x) + 1153	R^2 = 0.954
PN2	665	y = -50.3ln(x) + 1406	R^2 = 0.977
PN3	660	y = -38,2ln(x) + 1229	R^2 = 0.916
PN4	670	y = -51.7ln(x) + 1425	R^2 = 0.993

The specimens where fracture happen, had investigated the fracture surfaces at the vicinity of the fatigue crack initiation [15]. The graph of **Figure 3** shows the mean arithmetic deviations of the roughness profile Ra within the fish-eye crack area grown after 1.5 x 10^6 cycles.

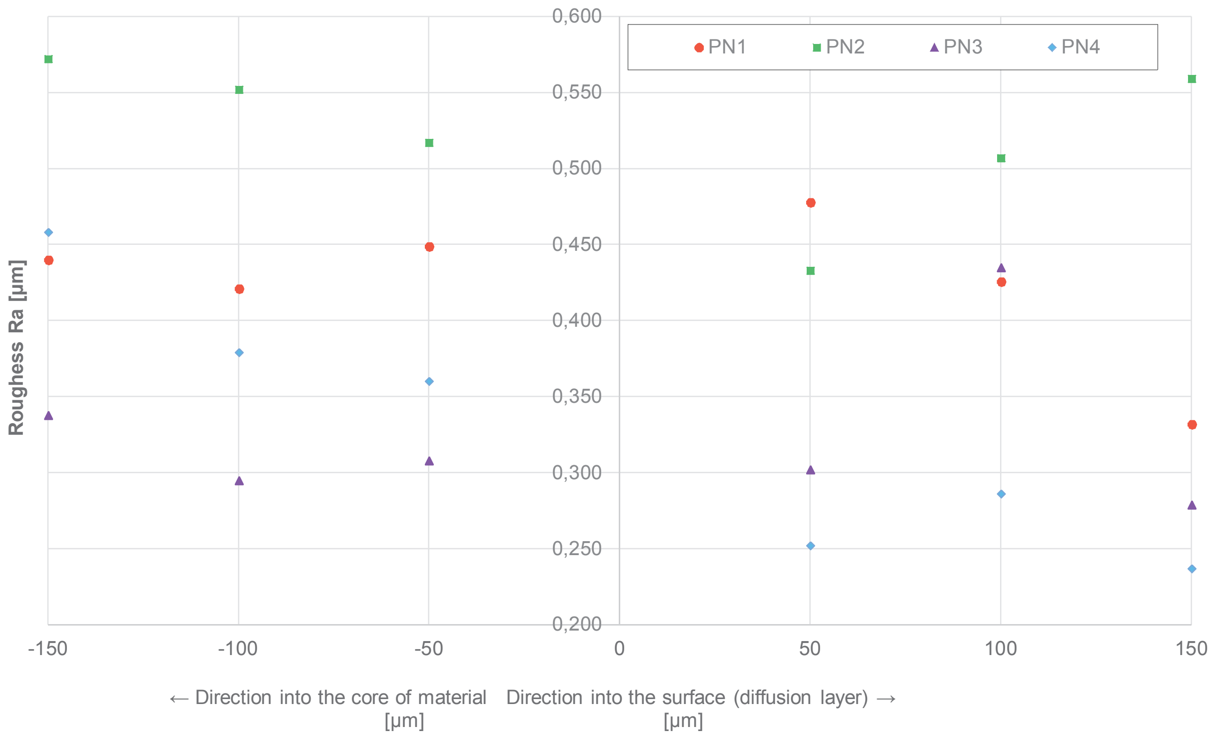

Figure 3 Common dependence of roughness on distance of measurements from inclusions

It is remarkable in case of base material to investigate the value of roughness. This value being the same for selected numbers of cycles 1.5 x 10^6 to fracture with one exception in case of PN2 series. When we observe direction to inclusion the roughness reduces and in its vicinity grows. On the other side of inclusion, in the direction to the diffusion layer, the dependence is analogous. From the inclusion to the diffusion layer is evident the difference in the overall decrease of roughness. The last measurement level was 150 μm from inclusion. In all series was reached comparable or smaller values of roughness with the mirror distance level from inclusion. After considering the measured values of roughness in fish-eye area could be obvious. A fatigue crack must overcome a barrier around inclusion. This barrier is lower to the diffusion layer and crack grows on quite uniformly. The value of cyclic load correlates with the value of the arithmetical mean deviation of roughness profile Ra. On the other side, direction to the core of material is a barrier predominantly formed by the thinning diffusion layer and gradually increasing proportion of the base material. A fatigue crack propagates worse. Roughness increase depending and is probably related with distance between the front of the crack and inclusion.

5. CONSLUSION

The conducted experiments show that fatigue characteristics of tested materials could rise by checking the formation of white layer. Ideally, complete elimination of the formation of the white layer by a proper adjustment of the plasma nitriding procedure conditions. To some extent, the optimal composition of the plasma nitriding atmosphere will depend on component specific application with the diffusion layer. Accordingly, the answer to the question of the process effectiveness is ensuing from a particular application. From this point of view, it is necessary to address also other key parameters applied in the process, among other things, process temperature and duration. The final thickness of the diffusion layer varies nonlinearly with increasing or decreasing these parameters.

For details describing the fatigue crack growth, roughness values were evaluated. The measurement was in close proximity to the inclusion. Distribution of roughness values around the inclusions apparently explains in a way the greater or lesser intensity of fatigue crack growth. This growth has meant in terms of overcoming physical barriers. When performing a more detailed analysis of the measured values of roughness. The characteristic of fatigue crack growth issue is usually convex shape of fish-eye towards into sample surface. The fish-eye area is geometrically characterized by an ellipsis. It's obvious that the fish-eye is with greater part located more in the diffusion layer than in the part which is nitrides poorer, i.e. in the base material.

There should be needed plentiful energy and time allowances for the process if emphasis is laid just on the permanent fatigue strength increase, whereat the way is in the complete elimination of the white layer. An appropriate composition of atmosphere will be richer in hydrogen and poorer in nitrogen.

ACKNOWLEDGEMENTS

The paper has been prepared thanks to the support of the project The Development of Technologies, Design of Firearms, Ammunition, Instrumentation, Engineering of Materials and Military Infrastructure "VÝZBROJ (DZRO K201)" and Surface technology in applications special techniques SV16-216.

REFERENCES

[1] POKORNÝ, Z., HRUBÝ, V. Plasma nitriding of deep narrow cavities. *Key engineering of materials*, 2011, vol. 465, p. 267-270. ISSN 1013-9826.

[2] STUDENY, Z., POKORNY, Z., DOBROCKY, D. Fatigue properties of steel after plasma nitriding proces. In *METAL 2016: 25th International Conference on Metallurgy and Materials*. Ostrava: TANGER, 2016, pp. 1175-1180. ISBN:978-80-87294-67-3. WOS: 000391251200191

[3] POKORNY, Z., KADLEC, J., STUDENY, Z., POSPICHAL, M., DOBROCKY, D. Solid state diffusion of nitrogen and carbon in the Fe-C system. In *METAL 2016: 25th International Conference on Metallurgy and Materials*. Ostrava: TANGER, 2016, pp. 1151-1156. ISBN:978-80-87294-67-3. WOS: 000391251200187

[4] ALP, T., WAZZAN, A. The influence of microstructure on the tensile and fatigue behavior of SAE 6150 steel. *Journal of Materials Engineering and Performance*, 11 (4), pp. 351-359. **ISSN:** 10599495DOI: 10.1361/105994902770343854

[5] OMORI, T., MORITA, T., OKADA, K., MAEDA, H. Improvement of fretting fatigue strength of stainless steel by hybrid surface treatment composed of plasma nitriding and fine-particle bombarding. *Nippon Kinzoku Gakkaishi/Journal of the Japan Institute of Metals*, 2016, vol. 80, Issue 4, pp. 225-230. **ISSN:** 00214876. **DOI:** 10.2320/jinstmet.J2015053

[6] KUFFOVA, M., BELLA, V. Fatigue resistance of magnesium alloy AZ 91D. Metallic materials, 2009, Vol. 47, Issue 6, p. 415-420

[7] STUDENÝ, Z. Analysis of the Influence of Initiating Inclusions on Fatigue Life of Plasma Nitrided Steels. *Manufacturing Technology*, 2015, vol. 15, no. 1, p. 99-105. ISSN 1213-2489.

[8] ČELKO, P., KUFFOVÁ, M., SHERMAN, A. Fatigue resistence of low-alloy steel post long-term plasma-nitriding. *Transactions of the Institute of Metal Finishing*, 2016, vol. 94, Issue 2, pp. 86-91. ISSN: 00202967. DOI: 10.1080/00202967.2015.1124637

[9] GENEL, K., DEMIRKOL, M., GÜLMEZ, T. Corrosion fatigue behaviour of ion nitrided AISI 4140 steel. *Materials Science and Engineering A*, 288 (1), pp. 91-100. DOI: 10.1016/S0921-5093(00)00835-2

[10] CSN 42 0363 Metal Testing. Fatigue Testing of Metals. Methodology of Testing.

[11] CSN 42 0368 Metal testing. Fatigue Testing of Metals. Statistical Evaluation of Fatigue Test Results of Metals.

[12] MANOVA, D., LUTZ, J., MANDL, S. Sputtering effects during plasma immersion ion implantation of metals. *Surface and Coatings Technology*, 2010, vol. 204, Issue 18-19, pp. 2875-2880. **ISSN:** 02578972

[13] VLČKOVA, I., JONŠTA, P., JONŠTA, Z., VÁŇOVÁ, P., KULOVÁ, T. Corrosion fatigue of austenitic stainless steels for nuclear power engineering. *Metals*, 2016, vol. 6, Issue 12, Article no. 319. ISSN: 20754701. **DOI:** 10.3390/met6120319

[14] MURAKAMI, Y. Metal Fatigue, Effect of Small Defects and Non-metallic Inclusions. *Elsevier publ.*, Oxford, UK (2002)

[15] DUBOVSKA, R., MAJERIK, J., CHOCHLIKOVA, H., BASKA, I. Residual stress measurement by X-ray diffraction method. In Annals of DAAAM and Proceedings of the International DAAAM Symposium, 2011, pp. 1327-1328. ISBN: 978-390150983-4.